J|A|C|S
ARTICLES
Published on Web 11/25/2004

Primary and Secondary Structure Dependence of Peptide Flexibility Assessed by Fluorescence-Based Measurement of End-to-End Collision Rates

Fang Huang,[†] Robert R. Hudgins,[†,‡] and Werner M. Nau*[,§]

Contribution from the Department of Chemistry, University of Basel, Klingelbergstrasse 80, CH-4056 Basel, Switzerland, and the School of Engineering and Science, International University Bremen, Campus Ring 1, D-28717 Bremen, Germany

Received June 9, 2004; E-mail: w.nau@iu-bremen.de

Abstract: The intrachain fluorescence quenching of the fluorophore 2,3-diazabicyclo[2.2.2]oct-2-ene (DBO) is measured in short peptide fragments, namely the two strands and the turn of the *N*-terminal β-hairpin of ubiquitin. The investigated peptides adopt a random-coil conformation in aqueous solution according to CD and NMR experiments. The combination of quenchers with different quenching efficiencies, namely tryptophan and tyrosine, allows the extrapolation of the rate constants for end-to-end collision rates as well as the dissociation of the end-to-end encounter complex. The measured activation energies for fluorescence quenching demonstrate that the end-to-end collision process in peptides is partially controlled by internal friction within the backbone, while measurements in solvents of different viscosities (H_2O, D_2O, and 7.0 M guanidinium chloride) suggest that solvent friction is an additional important factor in determining the collision rate. The extrapolated end-to-end collision rates, which are only slightly larger than the experimental rates for the DBO/Trp probe/quencher system, provide a measure of the conformational flexibility of the peptide backbone. The chain flexibility is found to be strongly dependent on the type of secondary structure that the peptides represent. The collision rates for peptides derived from the β-strand motifs (ca. 1×10^7 s^{-1}) are ca. 4 times slower than that derived from the β-turn. The results provide further support for the hypothesis that chain flexibility is an important factor in the preorganization of protein fragments during protein folding. Mutations to the β-turn peptide show that subtle sequence changes strongly affect the flexibility of peptides as well. The protonation and charge status of the peptides, however, are shown to have no significant effect on the flexibility of the investigated peptides. The meaning and definition of end-to-end collision rates in the context of protein folding are critically discussed.

Introduction

Protein folding is one of the "holy grails" of the physical and life sciences.[1−5] While several general folding mechanisms, such as the framework model, the hydrophobic collapse model, and the nucleation-condensation model, have been proposed,[1,4,6] the long-standing controversy on whether protein folding is kinetically or thermodynamically controlled has remained.[7−9] Studies of the elementary steps in protein folding, such as the formation of β-hairpins, α-helices, and loops, and in particular on the kinetics of the formation of these secondary structures are necessary to validate the various proposed folding mechanisms.[2,6] To better understand how the domains of a protein move, in which sequence a protein folds, and which secondary structures emerge first, it is essential to investigate peptide dynamics, to measure the kinetics of nonlocal intrachain interactions, and to predict the flexibility of peptide sequences.[2,10,11] For example, it may be anticipated that nucleation may occur near the conformationally most flexible (or most "dynamic") portions of a protein.

Recent studies show that the time scale of the elementary protein folding steps ranges from several nanoseconds to tens of microseconds. Such studies have included indirect dynamic NMR experiments[12,13] and direct photophysical intrastrand quenching experiments.[14−23] A critical parameter for protein

[†] University of Basel.
[‡] Present address: Department of Chemistry, York University, 4700 Keele Street, Toronto, ON, M3J 1P3 Canada.
[§] International University Bremen.

(1) Pain, R. H., Ed. *Mechanisms of Protein Folding*; 2nd ed.; Oxford University Press: Oxford, 2000.
(2) Eaton, W. A.; Munoz, V.; Hagen, S. J.; Jas, G. S.; Lapidus, L. J.; Henry, E. R.; Hofrichter, J. *Annu. Rev. Biophys. Biomol. Struct.* **2000**, *29*, 327−359.
(3) Brooks, C. L., III. *Acc. Chem. Res.* **2002**, *35*, 447−454.
(4) Daggett, V.; Fersht, A. R. *Trends Biochem. Sci.* **2003**, *28*, 18−25.
(5) Zhuang, X.; Rief, M. *Curr. Opin. Struct. Biol.* **2003**, *13*, 88−97.
(6) Volk, M. *Eur. J. Org. Chem.* **2001**, 2605−2621.
(7) Baker, D.; Agard, D. A. *Biochemistry* **1994**, *33*, 7505−7509.
(8) Baskakov, I. V.; Legname, G.; Prusiner, S. B.; Cohen, F. E. *J. Biol. Chem.* **2001**, *276*, 19687−19690.
(9) Cruzeiro-Hansson, L.; Silva, P. A. S. *J. Biol. Phys.* **2001**, *27*, S6−S9.
(10) Callender, R. H.; Dyer, R. B.; Gilmanshin, R.; Woodruff, W. H. *Annu. Rev. Phys. Chem.* **1998**, *49*, 173−202.
(11) Mayor, U.; Guydosh, N. R.; Johnson, C. M.; Grossmann, J. G.; Sato, S.; Jas, G. S.; Freund, S. M. V.; Alonso, D. O. V.; Daggett, V.; Fersht, A. R. *Nature* **2003**, *421*, 863−867.
(12) Wang, M.; Tang, Y.; Sato, S.; Vugmeyster, L.; McKnight, C. J.; Raleigh, D. P. *J. Am. Chem. Soc.* **2003**, *125*, 6032−6033.

Scheme 1. Structure of the N-terminal β-hairpin (1−17) of Ubiquitin (a) and General Structure of the Peptides Labeled with DBO/Trp (b) or DBO/Tyr (c)

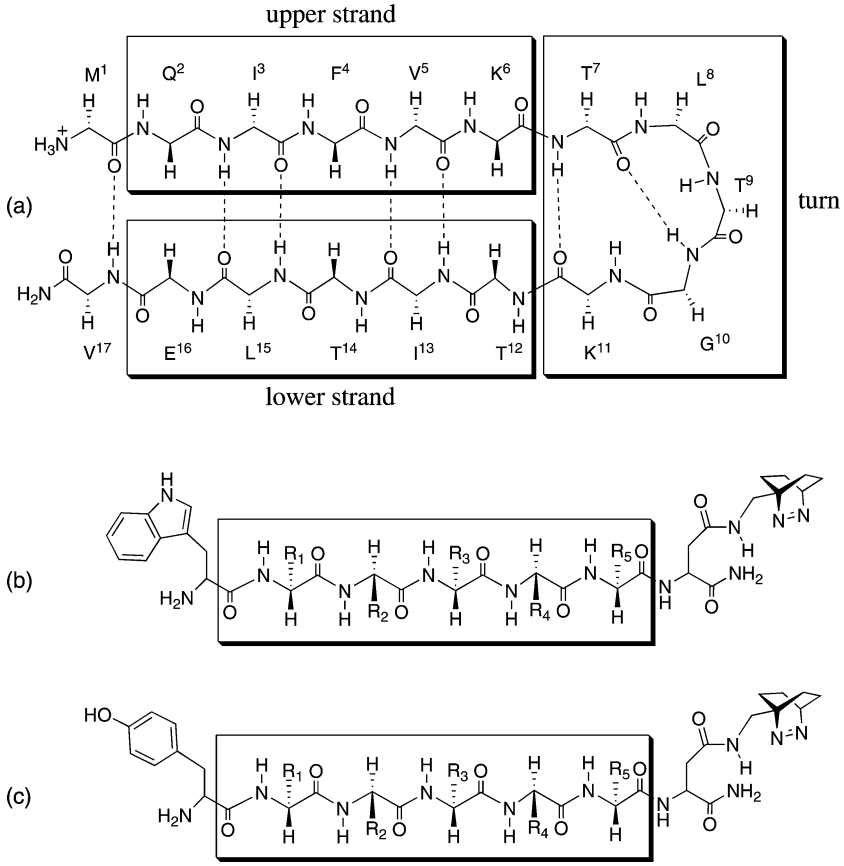

folding is the rate of intrachain collision, which imposes a rate limit for the formation of a loop or β-turn.[2,19,24] Recently, we have established a fluorescence-based method, with 2,3-diazabicyclo[2.2.2]oct-2-ene (DBO) as a probe and Trp as quencher, for measuring end-to-end collisions in biopolymers occurring on the submicrosecond time scale. The extremely long fluorescence lifetime of DBO, even in water under air, and its efficient contact quenching by Trp form the basis for its application to biopolymer dynamics. In addition, DBO is small, hydrophilic, and very versatile during peptide synthesis.[23,24]

The intramolecular fluorescence quenching of DBO by Trp has already proven useful to assess the length dependence of intrachain collisions,[23,25] and to determine the effect of the amino acid type on the flexibility of peptides.[24] The fundamental questions which we are addressing in the present study is how the flexibility of a peptide sequence depends on the secondary structure, how mutations of single amino acids affect the chain flexibility, how charge effects affect the end-to-end collision rates, and how the chain dynamics can be understood in terms of an interplay between solvent and internal friction. As an experimental model, we have selected a native sequence, the 17-residue *N*-terminal β-hairpin of ubiquitin, a small protein with 76 amino acids with well-investigated structure, stability, and folding behavior.[26−31] This hairpin, which is believed to play a key role in the early events of ubiquitin folding,[28,29] is composed of two β-strands connected by a β-turn as shown in Scheme 1.[29] To compare the sequence dependence of end-to-end collision rates and thereby assess the flexibility, we synthesized DBO/Trp or DBO/Tyr end-labeled peptides (Scheme 1b,c) derived from the "upper strand" (Q^2IFVK^6), the "lower strand" ($T^{12}ITLE^{16}$), and the "turn" (T^7LTGK^{11}) of the ubiquitin hairpin. These sequences are of interest because although they show random-coil behavior in solution, they represent structurally well-defined and distinct parts of the protein in the native, intact state.

(13) Huang, G. S.; Oas, T. G. *Proc. Natl. Acad. Sci. U.S.A.* **1995**, *92*, 6878−6882.
(14) Hagen, S. J.; Hofrichter, J.; Szabo, A.; Eaton, W. A. *Proc. Natl. Acad. Sci. U.S.A.* **1996**, *93*, 11615−11617.
(15) Hagen, S. J.; Hofrichter, J.; Eaton, W. A. *J. Phys. Chem. B* **1997**, *101*, 2352−2365.
(16) Munoz, V.; Thompson, P. A.; Hofrichter, J.; Eaton, W. A. *Nature* **1997**, *390*, 196−199.
(17) Thompson, P. A.; Eaton, W. A.; Hofrichter, J. *Biochemistry* **1997**, *36*, 9200−9210.
(18) Shastry, M. C. R.; Roder, H. *Nat. Struct. Biol.* **1998**, *5*, 385−392.
(19) Bieri, O.; Wirz, J.; Hellrung, B.; Schutkowski, M.; Drewello, M.; Kiefhaber, T. *Proc. Natl. Acad. Sci. U.S.A.* **1999**, *96*, 9597−9601.
(20) Lednev, I. K.; Karnoup, A. S.; Sparrow, M. C.; Asher, S. A. *J. Am. Chem. Soc.* **1999**, *121*, 4076−4077.
(21) Lapidus, L. J.; Eaton, W. A.; Hofrichter, J. *Proc. Natl. Acad. Sci. U.S.A.* **2000**, *97*, 7220−7225.
(22) Jas, G. S.; Eaton, W. A.; Hofrichter, J. *J. Phys. Chem. B* **2001**, *105*, 261−272.
(23) Hudgins, R. R.; Huang, F.; Gramlich, G.; Nau, W. M. *J. Am. Chem. Soc.* **2002**, *124*, 556−564.
(24) Huang, F.; Nau, W. M. *Angew. Chem., Int. Ed.* **2003**, *42*, 2269−2272.
(25) Yeh, I.-C.; Hummer, G. *J. Am. Chem. Soc.* **2002**, *124*, 6563−6568.
(26) Vijaykumar, S.; Bugg, C. E.; Cook, W. J. *J. Mol. Biol.* **1987**, *194*, 531−544.
(27) Weber, P. L.; Brown, S. C.; Mueller, L. *Biochemistry* **1987**, *26*, 7282−7290.
(28) Cox, J. P. L.; Evans, P. A.; Packman, L. C.; Williams, D. H.; Woolfson, D. N. *J. Mol. Biol.* **1993**, *234*, 483−492.
(29) Zerella, R.; Evans, P. A.; Ionides, J. M.; Packman, L. C.; Trotter, B. W.; Mackay, J. P.; Williams, D. H. *Protein Sci.* **1999**, *8*, 1320−1331.
(30) Bolton, D.; Evans, P. A.; Stott, K.; Broadhurst, R. W. *J. Mol. Biol.* **2001**, *314*, 773−787.
(31) Kitahara, R.; Akasaka, K. *Proc. Natl. Acad. Sci. U.S.A.* **2003**, *100*, 3167−3172.

The individual sequences should possess a different intrinsic flexibility and propensity for folding, which is reflected in the rate by which the two ends of the peptide collide. These intrinsic dynamic parameters of primary peptide sequences can be investigated in short sequences without the complications imposed by secondary structures, i.e., in the absence of any preferred, thermodynamically stable conformation. Since fast-folding turns are implicated as the initiators of the folding of β-hairpins, measuring the end-to-end collision rates of the turn and strand fragments of the β-hairpin may help to clarify the β-hairpin folding kinetics and mechanism.[16,32,33] These rates can be directly related to the intramolecular fluorescence quenching of DBO by either Trp or Tyr in the labeled sequences. The combination of these two quenchers with different quenching efficiencies allows the extrapolation of the microscopic rate constants for formation and dissociation of the end-to-end encounter complex, which itself presents a new methodology and extension of our fluorescence technique.[23]

Experimental Section

Materials. The synthesis of the Fmoc-protected and DBO-labeled asparagine derivative has been described previously.[23] Polypeptides (all amidated at the C-terminus) were made by Affina Immuntechnik (Berlin, Germany) in >95% purity (determined by MALDI-MS and HPLC). Water was bidistilled. D_2O (> 99.9% D) was from Glaser AG, Basel. Other commercial analytical-grade materials were from Fluka or Aldrich.

NMR and CD Measurements. NMR experiments were carried out on a Bruker DRX 500 spectrometer in D_2O (with 10% H_2O) at 1 mM peptide concentration. Circular dichroism (CD) experiments of the peptides were performed on a Jasco 720 circular dichroism spectrometer at ambient temperature at peptide concentrations of 10−100 μM.

Fluorescence Lifetime Measurements. Fluorescence lifetimes were measured on a laser flash photolysis setup (LP900, Edinburgh Instruments, Edinburgh, Scotland) with 7 mJ, 355-nm pulses of 4-ns width from a Nd:YAG laser (Minilite II, Continuum, Santa Clara, CA), and with a time-correlated single-photon counting fluorimeter (FLS920, Edinburgh Instruments) using a 1.5-ns pulse-width H_2 flash lamp at 365 nm. A solid-state diffuser was employed to obtain the instrument response function (IRF), which was used in the reconvolution procedure to obtain the fluorescence lifetimes. Fluorescence was detected at 430 nm.

Peptides were measured in H_2O and D_2O at ambient temperature unless stated differently. Typical concentrations of polypeptides were 10 μM for flash photolysis and 100 μM for single-photon counting experiments. The temperature-dependent experiments were carried out from 20 to 50 °C. The pH-dependent measurements were performed in phosphate buffer for pH 7, citrate/HCl/NaOH buffer for pH 2, and Na_2HPO_4/NaOH buffer for pH 12. The concentration of guanidinium chloride was adjusted by measuring the refractive index.

Results

NMR and CD Experiments. NMR and CD spectroscopy were carried out to corroborate that the investigated peptides adopt the random-coil conformation expected for such short sequences.[24,34] Assignments were based on a combination of 1D-NMR, 2D-COSY, and 2D-TOCSY spectra. The chemical shifts are very sensitive to the secondary structure,[35] which allows one to differentiate the random-coil structures from defined secondary structures. The chemical shifts obtained for all labeled peptides were compared with those reported for folded[27] as well as denatured[36] ubiquitin; see Table 1 for example. The chemical shifts of those residues which possess identical neighboring residues in the synthetic peptide fragments as in ubiquitin were not significantly different (±0.02 ppm) from those measured for denatured ubiquitin, i.e., in agreement with a random-coil conformation. Slight variances in chemical shift were expectedly observed for the residues *directly adjacent* to the probe or quencher, which experience an environment different from that in the denatured protein (upper and lower entry in Table 1).[34]

Table 1. ^{1}H NMR Chemical Shifts of the Labeled Turn Fragment (DBO-TLTGKY) in Comparison to Those in Denatured and Folded Ubiquitin

	δ(NH)/ppm			δ(αH)/ppm		
position	labeled peptide[a]	denatured ubiquitin[b]	folded ubiquitin[c]	labeled peptide[a]	denatured ubiquitin[b]	folded ubiquitin[c]
[T-7][d]	8.66	8.34	8.69	4.37	4.41	5.00
L-8	8.50	8.51	8.91	4.44	4.44	4.33
T-9	8.09	8.09	7.59	4.36	4.37	4.41
G-10	8.34	8.32	7.78	3.94	3.94	3.62/4.36[e]
[K-11][d]	8.17	8.10	7.25	4.18	4.09	4.37

[a] This work in D_2O with 10% H_2O. [b] At 8 M urea and pH 2, taken from ref 36. [c] At 50 °C in 25 mM acetic acid at pH 4.7, taken from ref 27. [d] Amino acid has a different direct neighbor in the labeled peptide and in ubiquitin. [e] Separate peaks for glycine α-protons.

CD measurements were also performed for all peptides at different pH values.[37] All CD spectra show the characteristic pattern for a random coil.[38,39] It is the combination of NMR and CD experiments, which allows us to exclude the existence of sizable amounts of secondary structure in the investigated peptides. All interpretations are therefore based on the assignment of random-coil behavior to the labeled peptide fragments.

Kinetics of End-to-End Collision in the Turn and Strand Peptides. The fluorescence-based method for measuring the end-to-end collision rate constants in peptides has been discussed in detail.[23] The intramolecular quenching rate constant in a probe/quencher-labeled peptide is first obtained according to eq 1 from the experimental fluorescence lifetimes of the probe-labeled peptides with (τ) and without (τ_0) an attached quencher.

The quenching rate constant is a composite of the microscopic rate constants in Scheme 2 and can be expressed by eq 2, which employs the common steady-state approximation for the formation of the end-to-end encounter complex. k_+ is the end-to-end collision rate constant to form the probe/quencher encounter complex and k_- and k_d are the rate constants for its dissociation and deactivation, respectively. For a diffusion-controlled reaction $k_d \gg k_-$ applies and the simplified eq 3 results, i.e., for a diffusion-controlled probe/quencher pair the end-to-end collision rate constant equals directly the experimental quenching rate

(32) Klimov, D. K.; Thirumalai, D. *Proc. Natl. Acad. Sci. U.S.A.* **2000**, *97*, 2544−2549.
(33) Wang, H.; Sung, S.-S. *J. Am. Chem. Soc.* **2000**, *122*, 1999−2009.
(34) Schwarzinger, S.; Kroon, G. J. A.; Foss, T. R.; Chung, J.; Wright, P. E.; Dyson, H. J. *J. Am. Chem. Soc.* **2001**, *123*, 2970−2978.
(35) Wishart, D. S.; Sykes, B. D.; Richards, F. M. *J. Mol. Biol.* **1991**, *222*, 311−333.
(36) Peti, W.; Smith, L. J.; Redfield, C.; Schwalbe, H. *J. Biomol. NMR* **2001**, *19*, 153−165.
(37) The application of CD as an alternative technique to NMR was warranted since Maynard et al. have suggested that the relevant chemical shifts only occur when the full β-hairpin of ubiquitin is present, while the β-strand alone may give almost random-coil-like values for the ^{1}H chemical shifts; cf. Maynard, A. J.; Sharman, G. J.; Searle, M. S. *J. Am. Chem. Soc.* **1998**, *120*, 1996−2007. The authors further suggested that the $^3J_{\alpha N}$ coupling constants may be a better indicator for secondary structure, which were not determined in the present work.
(38) Woody, R. W. *Adv. Biophys. Chem.* **1992**, *2*, 37−79.
(39) Greenfield, N. J. *Anal. Biochem.* **1996**, *235*, 1−10.

Table 2. Fluorescence Lifetimes, Quenching Rate Constants, and Solvent Deuterium Isotope Effects for the Intramolecular and Intermolecular Quenching of DBO-Labeled Peptides and DBO by Tryptophan and Tyrosine

		in H_2O		in D_2O		
fragment	sequence	τ/ns	k_q[a]/(10^6 s^{-1})	τ/ns	k_q[a]/(10^6 s^{-1})	$k_q(H_2O)/k_q(D_2O)$
upper strand	WQIFVK-DBO	90	8.2	110	7.1	1.2
	YQIFVK-DBO	172	3.0	266	1.8	1.7
lower strand	WTITLE-DBO	63	13.0	74	12.0	1.1
	YTITLE-DBO	110	6.1	175	3.9	1.6
	[YELTIT-DBO][b]	126	5.0	215	2.8	1.8
turn	WTLTGK-DBO	27	34.0	33	28.0	1.2
	YTLTGK-DBO	74	10.2	130	5.6	1.8
	[DBO-TLTGKY][c]	76	9.9	135	5.3	2.0
intermolecular	W + QIFVK-DBO		1600 M^{-1}		1400 M^{-1}	1.1
	Y + QIFVK-DBO		230 M^{-1}		130 M^{-1}	1.8
	W + DBO		2100 M^{-1}		2000 M^{-1}	1.1
	Y + DBO (pH 7)		560 M^{-1}		360 M^{-1}	1.6
	Y + DBO (pH 12)		2100 M^{-1}		1800 M^{-1}	1.2

[a] Unless stated differently, lifetimes of corresponding peptides without quencher were taken as τ_0 in the calculation of intramolecular quenching rate constants according to eq 1; estimated errors in lifetimes and quenching rate constants are 5% (10% for intermolecular values). [b] Inverted lower strand; lifetime of TITLE-DBO taken as τ_0. [c] Probe/quencher-exchanged turn; lifetime of TLTGK-DBO taken as τ_0.

Scheme 2. Kinetic Scheme for Intramolecular Fluorescence Quenching

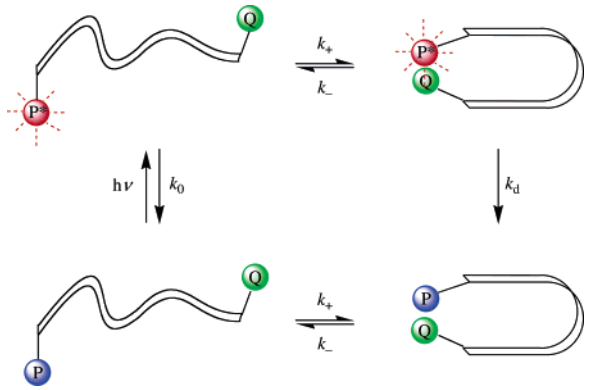

constant. For a nondiffusion-controlled system, interpretations must be based on eq 2. In the present work, Trp was employed as an essentially diffusion-controlled quencher of DBO and Tyr, as a nondiffusion-controlled quencher.

$$k_q = \frac{1}{\tau} - \frac{1}{\tau_0} \quad (1)$$

$$k_q = \frac{k_+ k_d}{k_- + k_d} \quad (2)$$

$$k_q \approx k_+ \text{ for } k_d \gg k_- \quad (3)$$

The three peptide fragments without quencher, TLTGK-DBO, QIFVK-DBO, and TITLE-DBO, displayed fluorescence lifetimes of 480, 510, and 540 ns in D_2O, respectively. These fluorescence lifetimes are similar to that of parent DBO (505 ns), indicating that a peptide composed of inert amino acids does not significantly quench DBO.[23] The attachment of Trp or Tyr as quencher reduced the lifetimes substantially. From the quenching effects the intramolecular quenching rate constants were obtained according to eq 1 (Table 2). When Tyr is used as quencher, the peptide corresponding to the β-turn (YTLTGK-DBO) gives the fastest fluorescence quenching rate, the one corresponding to the upper strand (YQIFVK-DBO) displays approximately a 4 times slower quenching rate, and the rate for the lower strand peptide (YTITLE-DBO) lies in between.[40] Substitution of Tyr by Trp (Table 2) results in much shorter fluorescence lifetimes and accordingly higher quenching rate constants, around 3−5-fold higher. In contrast, measurements in more viscous[41] guanidinium chloride solutions (Table 3) lead to a decrease in rate constants by a factor of 2−3. However, regardless of the variation in the absolute rate constants, the order of the quenching efficiency remains the same for both quenchers, i.e., β-turn > lower strand > upper strand. Shown in Figure 1 are representative fluorescence decay traces.

The intramolecular fluorescence quenching is induced by a collision between probe and quencher, which occurs with a different frequency depending on the flexibility of the peptide backbone. The quenching rate constants can therefore be interpreted in terms of the peptide flexibility;[23,24] i.e., the turn sequence of ubiquitin is more flexible than the two strand sequences.

Activation Energy of End-to-End Collision. The activation energies for intramolecular end-to-end collision in probe/quencher-labeled peptides were obtained by plotting the temperature dependence of the quenching rate constants. For this purpose, the fluorescence lifetimes were measured for each peptide with and without quencher at different temperatures, and the quenching rate constants were then individually determined for each temperature according to eq 1. In the absence of quenchers, the fluorescence lifetime of DBO shows a very weak temperature dependence.[42] The variation in the fluorescence lifetime of the DBO-labeled peptides without quencher was therefore much weaker than that of the peptides with quencher attached, which indicated a sizable activation barrier for the quenching process. All Arrhenius plots were linear; see Figure 2 for example.

Notably, the experimental activation energies for intramolecular quenching in aqueous solution (17−25 kJ mol^{-1}, Table 3) are similar to or larger than the apparent activation energy of solvent viscous flow in the same temperature range

(40) For consistency, all peptides were labeled with DBO at the C-terminus. A control experiment with the turn-derived peptide DBO-TLTGKY, where the terminal positions of probe and quencher are exchanged but where the peptide backbone remains the same, yielded the same quenching rate constant within error as the YTLTGK-DBO peptide (Table 2), which supports the idea that the measured quenching rates reflect an intrinsic dynamic property of the peptide backbone, namely its flexibility.
(41) Kawahara, K.; Tanford, C. *J. Biol. Chem.* **1966**, *241*, 3228−3232.
(42) Nau, W. M.; Greiner, G.; Rau, H.; Wall, J.; Olivucci, M.; Scaiano, J. C. *J. Phys. Chem. A* **1999**, *103*, 1579−1584.

Table 3. End-to-End Collision Rates and Activation Energies of DBO/Trp-Labeled Peptides in Different Solvents[a]

fragment	sequence	solvent[b]	$k_q/(10^6\ s^{-1})$	$\ln(A/s^{--1})$	E_a/(kJ mol^{-1})
upper strand	WQIFVK-DBO	H_2O	8.2	25.5	23
		D_2O	7.1	25.5	25
		4.4 M Gdn.HCl	6.7		
		7.0 M Gdn.HCl	3.8	26.8	29
lower stand	WTITLE-DBO	H_2O	13.0	25.0	21
		D_2O	12.0	24.5	20
		4.4 M Gdn.HCl	9.5		
		7.0 M Gdn.HCl	4.6	27.4	28
turn	WTLTGK-DBO	H_2O	34.0	24.0	17
		D_2O	28.0	24.0	17
		4.4 M Gdn.HCl	22.0		
		7.0 M Gdn.HCl	12.2	25.8	23

[a] To obtain the intramolecular quenching rate constant at different temperatures (298−328 K), the lifetime of the corresponding peptide without quencher was measured at the same temperature and taken as τ_0. Error in k_q is 5% and in $E_a \pm 1$ kJ mol^{-1}. [b] The viscosities of the solvents at 25 °C are 0.89 cP in H_2O, 1.10 cP in D_2O, 1.18 cP in 4.4 M Gdn.HCl, and 1.71 cP in 7.0 M Gdn.HCl.

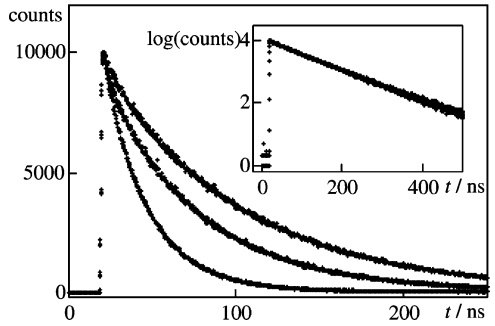

Figure 1. Fluorescence decays (measured by single-photon counting) of ubiquitin-derived peptides (100 μM in D_2O). The traces derive from the upper strand (WQIFVK-DBO, upper trace), lower strand (WTITLE-DBO, middle trace), and the turn (WTLTGK-DBO, lower trace). Shown in the inset is the decay for WQIFVK-DBO on a semilogarithmic scale.

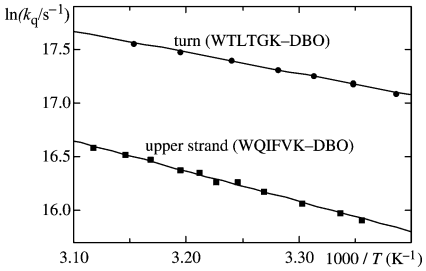

Figure 2. Representative Arrhenius plots for the intramolecular fluorescence quenching in DBO-labeled peptides by Trp.

(298−328 K), which amounts to 15.5 kJ mol^{-1} for H_2O and 16.6 kJ mol^{-1} for D_2O.[43] Activation energies in the same range have been reported for intrachain collision in a larger unfolded protein.[44] For comparison, the activation energies for the bimolecular quenching of a DBO-labeled peptide (QIFVK-DBO) by the free quenchers, Trp and Tyr, fell in the range 15 $\pm$ 3 kJ mol^{-1} in deaerated H_2O and D_2O; these intermolecular values have a larger error due to the small amount of quenching even at the solubility limit of Tyr and Trp. Note also that the difference in the activation energy of viscous flow between D_2O and H_2O (ca. 1 kJ mol^{-1}) is too small to result in experimentally significant effects on the activation barriers. In contrast, the selection of 7.0 M guanidinium chloride solution as a substantially more viscous solvent causes a pronounced increase in the activation energies for intramolcular quenching (Table 3).

The order of the activation energies follows the order of the end-to-end collision rates, i.e., the most flexible β-turn peptide (TLTGK) displays the lowest activation energy, and the upper, most rigid β-strand peptide shows the highest activation barrier. Accordingly, end-to-end collision is energetically facilitated in the β-turn peptide compared to the β-strand peptides. The fact that some activation barriers exceed the value expected for viscous flow in water immediately indicates that the end-to-end collision process is slowed not only by "solvent friction" but also by an "internal friction" (to employ the terminology of polymer models). In other words, some residues impose sizable barriers for those conformational rearrangements of the peptide backbone, which are required to bring the chain ends into contact.

Importantly, the values of the activation energies in the different peptides are the same, within error, for both Trp (Table 3) and Tyr (data not shown) as quencher. This result is consistent with the notion that the experimental activation energies for the intramolecular reaction are dominated by the backbone properties, i.e, an interplay of internal friction (flexibility of the peptide backbone) and solvent friction (viscosity-dependent diffusional motion). The lower intramolecular quenching efficiency of Tyr (Table 2) is therefore mainly manifested in a reduced preexponential A factor, as expected from the very different transition states for quenching (see below).

The trend of the preexponential A factors with the type of peptide fragment (Table 3) is less intuitively understood. However it can at least be demonstrated that the *order of magnitude* is reasonable for an intramolecular reaction by comparison with the theoretical relationship for an ideal (Gaussian) chain and an ideal intermolecular collision in eq 4, which assumes the same activation barrier for both processes.[45]

$$\frac{A^{\text{intra}}}{A^{\text{inter}}} \approx \left(\frac{3}{2\pi N b^2 N_a}\right)^{3/2} \qquad \text{(ideal behavior)} \qquad (4)$$

N represents the number of chain segments, N_a, the Avogadro number, and b, the length of one segment. For a heptapeptide ($N = 7$) with a length of 3.8 Å for each peptide bond,[15] A^{intra}, the preexponential factor of an intramolecular reaction, should

(43) Cho, C. H.; Urquidi, J.; Singh, S.; Robinson, G. W. *J. Phys. Chem. B* **1999**, *103*, 1991−1994.
(44) Hagen, S. J.; Carswell, C. W.; Sjolander, E. M. *J. Mol. Biol.* **2001**, *305*, 1161−1171.
(45) Nau, W. M.; Huang, F.; Wang, X.; Bakirci, H.; Gramlich, G.; Marquez, C. *Chimia* **2003**, *57*, 161−167.

Table 4. Intrinsic Fluorescence Lifetimes[a] of the DBO-Labeled Reference Peptides and DBO in the Absence of Tryptophan and Tyrosine as Quenchers at Different pH in H_2O

		τ/ns		
fragment	sequence	pH 2	pH 7	pH 12
upper strand	QIFVK-DBO	355	355	240
lower strand	TITLE-DBO	350	340	320
turn	TLTGK-DBO	315	305	205
intermolecular	DBO	315	320	315

[a] Error in lifetimes is ±10 ns.

then amount to approximately 50% of the value for the corresponding intermolecular reaction, A^{inter}. One therefore expects the preexponential factors for the intramolecular reactions to fall below those for the intermolecular processes ($\ln A \approx 26$ for quenching of QIFVK-DBO by Trp or Tyr). The experimental results in Table 3 are in agreement with this notion, although the decrease is quite pronounced for some peptides, which points to strong deviations from ideal-chain behavior.

Charge Effects. The effects of charge on the end-to-end collision process in the peptides derived from ubiquitin were also investigated through pH control as well as positional mutation in the peptides. Shown in Table 4 is the pH dependence of the lifetimes for free DBO and the peptides without quencher. The lifetime of DBO remains constant from pH 2−12. Peptides without quencher also have the same lifetime within error at pH 2 and pH 7, but their fluorescence lifetimes decreased at pH 12, especially for QIFVK-DBO and TLTGK-DBO. This decrease is related to the deprotonation of the photochemically inert aminium groups at the N-terminus and in particular in lysine to produce reactive amino groups; amines are well-known quenchers of DBO fluorescence (through exciplex formation),[46] which accounts for the decrease in fluorescence lifetime, most pronounced in peptides containing lysine, at very alkaline pH. For comparison, the intermolecular quenching rate constant for DBO by lysine increases from $\leq 1 \times 10^6\ M^{-1}\ s^{-1}$ at acidic and neutral pH[23] to $1.45 \times 10^7\ M^{-1}\ s^{-1}$ at pH 12 (this work). Note that the intrachain quenching by other amino acids but Tyr and Trp is explicitly corrected for in eq 1 by the proper choice of τ_0.

The charge effects on the quenching rate constants for the peptides with quencher are contained in Table 5. Strikingly, quenching for all Tyr peptides increases significantly at high pH. This increase, however, is not indicative for an effect on the chain dynamics but due to the deprotonation of tyrosine itself, which produces the phenoxyl anion, a stronger quencher of DBO fluorescence. Note that while the *intermolecular* quenching rate constant of DBO by Trp is independent of pH, that by Tyr increases by a factor of 4 between pH 7 and 12 (Table 2). There appears to be a change in quenching mechanism by tyrosine from hydrogen abstraction[23] for the phenol form at pH 7 to exciplex formation for the phenolate ion at pH 12. This is reflected in the decrease in solvent isotope effect from 1.6 at pH 7 to 1.2 at pH 12 (Table 2); the isotope effect at pH 7 is related to a partially reaction-controlled abstraction of the solvent-exchangeable phenolic hydrogen atom, while the minor isotope effect at pH 12 can be accounted for in terms of the viscosity-related solvent isotope effect on a close to diffusion-controlled reaction, akin to the minor solvent isotope effect observed for Trp (Table 2).

Due to the variation of the quenching rate constants, the tyrosine peptides studied at pH 12 should be treated separately. Note, however, that Tyr at pH 12 has (incidentally) the same quenching rate constant as Trp. Since the intramolecular quenching of DBO by Trp is presumed to be essentially diffusion-controlled, the same should apply for tyrosine at pH 12. In fact, the rate constants for all Tyr-labeled peptides at pH 12 are equal, within error, to the corresponding Trp-labeled sequences (Table 5).

Mutation Effects. Numerous studies in the area of protein engineering have demonstrated that specific amino acids can have a substantial effect on the folding, structure, stability, and function of proteins.[48−51] We have therefore investigated mutation effects of a *single* amino acid on the flexibility of the β-turn peptide derived from ubiquitin (Table 6). The different mutants show very different quenching rate constants, which confirms the importance of individual amino acids in determining peptide chain flexibility.

Discussion

We have investigated the end-to-end collision rates of equally long peptides derived from the N-terminal β-hairpin of ubiquitin, which report on the flexibility in dependence on the primary structure and secondary structure propensity of the peptides. The intrachain dynamics was studied by measuring the intramolecular fluorescence quenching rate constants between DBO, attached as fluorophore to the C-terminus, and either Trp or Tyr, attached as quenchers to the N-terminus (Scheme 1b,c). Due to the nearly diffusion-controlled quenching of excited DBO by Trp, the corresponding quenching rate constants have been proposed to be approximately equal to the end-to-end collision rate constants.[23,25] Tyr presents also a good, albeit nondiffusion-controlled quencher among the 20 amino acids.[23] Tyr was selected as a complementary quencher to investigate the quantitative effect of nondiffusion-controlled *intermolecular* quenching on the *intramolecular* quenching rate,[23] to extrapolate to the fully diffusion-controlled end-to-end collision rates (k_+), and to estimate the dissociation rates of the end-to-end encounter complex (k_- in Scheme 2).

Primary and Secondary Structure Dependence of Peptide Flexibility. The quenching rate constants for the three peptide fragments derived from the ubiquitin β-hairpin have been determined for both the DBO/Trp and the DBO/Tyr probe/quencher pair. All investigated peptides adopt a random-coil conformation as established by NMR and CD, which allows one to relate the efficiency of intramolecular quenching to the dynamics of the intrachain motion rather than to a structural preference or spatial proximity between probe and quencher. Both sets of data (for Trp and Tyr as quencher) reveal the same order of quenching rates and therefore flexibility of the peptide sequence: turn > lower strand > upper strand. For example,

(46) Pischel, U.; Zhang, X.; Hellrung, B.; Haselbach, E.; Muller, P.-A.; Nau, W. M. *J. Am. Chem. Soc.* **2000**, *122*, 2027−2034.
(47) Mathews, C. K.; van Holde, K. E.; Ahern, K. G. *Biochemistry*; 3rd ed.; Benjamin/Cummings: San Francisco, 2000.
(48) Vendruscolo, M.; Pacl, E.; Dobson, C. M.; Karplus, M. *Nature* **2001**, *409*, 641−645.
(49) Brannigan, J. A.; Wilkinson, A. J. *Nat. Rev. Mol. Cell Biol.* **2002**, *3*, 964−970.
(50) Goldenberg, D. P. *Annu. Rev. Biophys. Biophys. Chem.* **1988**, *17*, 481−507.
(51) Waldburger, C. D.; Jonsson, T.; Sauer, R. T. *Proc. Natl. Acad. Sci. U.S.A.* **1996**, *93*, 2629−2634.

Table 5. Charge Effects on the Rate Constants for the Intramolecular and Intermolecular Fluorescence Quenching of DBO-Labeled Peptides and DBO in Dependence on pH in H_2O

		$k_q/(10^6\ s^{-1})$ [a] charge status [b]		
fragment	sequence	pH 2	pH 7	pH 12
upper strand	WQIFVK–DBO	7.2 $^{+}$ $^{+}$ WQIFVK-DBO	8.2 $^{+}$ $^{+}$ WQIFVK-DBO	7.1 WQIFVK-DBO
	YQIFVK–DBO	2.8 $^{+}$ $^{+}$ YQIFVK-DBO	3.0 $^{+}$ $^{+}$ YQIFVK-DBO	6.7 $^{-}$ YQIFVK-DBO
lower strand	WTITLE–DBO	11.0 $^{+}$ WTITLE-DBO	13.0 $^{+}$ $^{-}$ WTITLE-DBO	15.0 $^{-}$ WTITLE-DBO
	YTITLE–DBO	5.8 $^{+}$ YTITLE-DBO	6.1 $^{+}$ $^{-}$ YTITLE-DBO	16.0 $^{-}$ $^{-}$ YTITLE-DBO
	[YTITLK–DBO] [c]	4.5 $^{+}$ $^{+}$ YTITLK-DBO	4.4 $^{+}$ $^{+}$ YTITLK-DBO	13.0 $^{-}$ YTITLK-DBO
	[YELTIT–DBO] [d]	4.6 $^{+}$ YELTIT-DBO	5.0 $^{+-}$ YELTIT-DBO	16.0 $^{- -}$ YELTIT-DBO
turn	WTLTGK–DBO	30.0 $^{+}$ $^{+}$ WTLTGK-DBO	34.0 $^{+}$ $^{+}$ WTLTGK-DBO	35.0 WTLTGK-DBO
	YTLTGK–DBO	9.8 $^{+}$ $^{+}$ YTLTGK-DBO	10.2 $^{+}$ $^{+}$ YTLTGK-DBO	31.0 $^{-}$ YTLTGK-DBO
	[DBO–TLTGKY] [e]	10.0 $^{+}$ $^{+}$ DBO-TLTGKY	9.9 $^{+}$ $^{+}$ DBO-TLTGKY	34.0 $^{-}$ DBO-TLTGKY
intermolecular	W + DBO	1800 M^{-1} $^{+}$ DBO + W	2000 M^{-1} DBO + W	2300 M^{-1} $^{-}$ DBO + W
	Y + DBO	600 M^{-1} $^{+}$ DBO + Y	560 M^{-1} DBO + Y	2100 M^{-1} $^{- -}$ DBO + Y
	K + DBO	≤1 M^{-1} $^{++}$ DBO + K	≤1 M^{-1} $^{+}$ DBO + K	14.3 M^{-1} $^{-}$ DBO + K

[a] Reference values (τ_0) were individually determined for corresponding peptide without quencher; estimated error is 5%. [b] Charge status based on the pK_a values reported in ref 47. Positive charges for N-terminal amino acids refer to protonated amino groups; note that the C-terminus is amidated in all synthetic peptides and remains uncharged. [c] Mutated lower strand; lifetime of TLTGK-DBO taken as τ_0. [d] Inverted lower strand; lifetime of TITLE-DBO taken as τ_0. [e] Probe/quencher-exchanged turn; lifetime of TLTGK-DBO taken as τ_0.

the quenching rate constant for the turn peptide (TLTGK) is 2−4 times faster than that of the peptides corresponding to the upper and lower strand (QIFVK and ELTIT). The spectroscopic measurements suggest that the β-turn region of ubiquitin is "more flexible" than the β-strand regions. This notion is also supported by the activation energy for end-to-end collision, which is significantly (up to 8 kJ mol^{-1}) lower for the β-turn than for both β-strands (Table 3). Indeed, the TLTGK turn has been suggested to be highly flexible even in the structure of native ubiquitin.[26] The fact that TLTGK is more flexible and can form a turn much faster than the other examined peptides may play an important role in the early events of ubiquitin folding. In terms of protein folding, one may argue that there is a clear kinetic bias toward *N*-terminal β-hairpin folding, in addition to a thermodynamic driving force. Obviously, a flexible region in a protein is more likely to serve as a nucleus for the formation of the secondary structure.

Variations in the distance distribution are known to cause significant effects on end-to-end collision rates, e.g., when the backbone is elongated by two or more amino acids.[19,21,23] The investigated peptide fragments have therefore been selected to be equally long in order to ensure comparable distance distribu-

Table 6. Mutation Effects on the Rate Constants for Intramolecular Fluorescence Quenching of the DBO-Labeled Turn Peptide by Tyrosine as N-Terminal Quencher

		in H_2O		in D_2O	
mutation	sequence	τ/ns	$k_q^a/(10^6\ s^{-1})$	τ/ns	$k_q^a/(10^6\ s^{-1})$
none	YTLTGK-DBO	74	10.2	130	5.6
G→A	YTLT*A*K-DBO	108	6.1	164	4.1
G→F	YTLT*F*K-DBO	110	6.0	168	4.0
G→T	YTLT*T*K-DBO	112	5.8	185	3.4
G→V	YTLT*V*K-DBO	138	4.1	220	2.5
T→G	YTL*G*GK-DBO	68	11.6	120	6.3

[a] τ_0 was taken as 325 ns in H_2O and 500 ns in D_2O; estimated errors in lifetimes and quenching rate constants are 5%.

tions. FRET experiments[52] further indicate that the average end-to-end distances are similar in the three peptide fragments (10.4 ± 0.6 Å), characteristic for random-coil pentapeptide backbones. The strong variation in the end-to-end collision rates of the peptides is therefore presumed to have its underlying reasons *not* in differential distance distributions but in the chain dynamics, i.e., the flexibility of the backbone as imposed by the specific amino acid sequence. As shown in a preliminary communication, individual amino acids affect the flexibility of peptides to a different extent with the flexibility order being as follows:[24] Gly > Ser > Asp, Asn, Ala > Thr, Leu > Phe, Glu, Gln > His, Arg > Lys > Val > Ile > Pro. This scale was established for peptide backbones composed of six identical amino acids, such that a direct comparison with the mixed ubiquitin sequences is difficult. However, it is reasonable to assume that the high flexibility of the TLTGK turn region is mainly due to the presence of the most flexible Gly unit, while the high rigidity of the TITLE and, more pronounced, the QIFVK strand is mainly imposed by the presence of one or two very rigid β-branched isoleucine and valine segments, respectively. To verify this intuition, the effect of mutations on the β-turn region was investigated.

In a first set of experiments, Gly in the TLTGK β-turn was mutated to Ala, Phe, Thr, and Val to demonstrate its importance in determining the flexibility of this fragment. Indeed, the quenching rate constants (studied for the DBO/Tyr probe quencher pair, Table 6) decreased significantly in the order Gly > Ala, Phe, Thr > Val, suggesting an increase in rigidity. This increase is in line with expectations from the flexibility scale (see above) yet somewhat less pronounced than that in the preliminary study,[24] since only a single amino acid was exchanged. Note again that variations in hydrophobicity of the residues have no systematic effect on the flexibility of the peptide mutants, in agreement with our previous study on peptide homopolymers.[24]

The rate constants for the Ala, Phe, and Thr mutants resemble those observed for the lower strand, while the rate constant for the Val mutant even approaches the rate measured for the upper strand (Table 2 and Table 6). This result demonstrates that the Gly in the turn sequence is indispensable for the high flexibility, while the β alkyl-branched residues substantially increase the rigidity in the strands. The latter have, in fact, also a high propensity to occur in β-strands, while Gly is a prominent amino acid in β-turn regions.[53−56] The β alkyl-branched residues may predispose these sequences to be relatively extended and rigid, which does, along with the high flexibility of the β-turn region, essentially predefine the formation of a β-hairpin. The β-hydroxyl-branched Thr appears more flexible than the β-alkyl-branched amino acids Val and Ile.[24] In contrast to Val and Ile, Thr has also a high propensity to occur in β-turns, in addition to β-sheets.[53−56] The higher flexibility of Thr is reflected in the larger quenching rate constant of the G→T mutant compared to the G→V mutant (Table 6).

The mutation of an additional amino acid adjacent to the presumably most flexible Gly linkage, namely of T→G to give TLGGK, causes an additional increase in chain flexibility (Table 6), which is in line with expectations based on the individual flexibility of the amino acids.[24] However, it appears unlikely that effects related to chain flexibility are simply additive or predictable in an incremental fashion. Rather, specific amino acids and specific positions as well as the particular sequence are all expected to affect the internal friction in a peptide, and they may be vital to produce a flexible peptide, which requires more detailed follow-up work.[40] For example, we have designed an inverse sequence of the lower strand peptide in which the amino acid composition is the same but in which the sequence is inverted from TITLE (original) to ELTIT (inverted). The results (Table 2) revealed a significant sequence effect (ca. 20−30%) on the fluorescence quenching rate constant, which demonstrates the limitations of predicting chain flexibility in an incremental fashion.

The experimental data for the two β-strands suggest a somewhat higher flexibility of the lower strand (Table 2), which is presumably related to the presence of an additional β-alkyl branched amino acid in the upper strand. However, in the actual β-hairpin of ubiquitin both strands could display a comparable rigidity. Note that the present studies were limited to pentameric β-strand sections of the β-hairpin (Q^2IFVK^6 and $T^{12}ITLE^{16}$) in order to allow a direct comparison to the intervening pentameric β-turn fragment (T^7LTGK^{11}). The inclusion of the additional residues of the β-strands, i.e., the comparison of the hexamers M^1QIFVK^6 and $T^{12}ITLEV^{17}$ (see Scheme 1), should give rise to similarly rigid strand fragments, since a stiffening β-branched Val residue is added to the lower strand.

We also questioned to which degree a variation in the charge status of the different peptide fragments could be responsible for the observed variations in end-to-end collision rates. Much effort has therefore been devoted to the design of pH-dependent experiments (Table 5) to scrutinize the existence of charge effects on the end-to-end collision rates. In addition, we used a peptide sequence with a Glu → Lys mutation to invert the charge status within the same sequence through the exchange of an acidic for a basic site (YTITLE-DBO and YTITLK-DBO in Table 5). However, the combined experiments did not yield a systematic dependence on the charge status.

We conclude from Table 5 that any effects related to the repulsion or attraction of two charges are too minute to result in experimentally significant effects on the end-to-end collision rates (<10%). In fact, in our preliminary communication only a small charge effect on the end-to-end collision rates (ca. 10%) became observable even with six charged residues.[24] The important conclusion in regard to end-to-end collision rate constants for the three ubiquitin-derived peptide fragments is

(52) Sahoo, H.; Huang, F.; Meyer, R.; Nau, W. M. Unpublished results.

(53) Levitt, M. *Biochemistry* **1978**, *17*, 4277−4285.
(54) Hutchinson, E. G.; Thornton, J. M. *Protein Sci.* **1994**, *3*, 2207−2216.
(55) Muñoz, V.; Serrano, L. *Proteins* **1994**, *20*, 301−311.
(56) Koehl, P.; Levitt, M. *Proc. Natl. Acad. Sci. U.S.A.* **1999**, *96*, 12524−12529.

Table 7. Extrapolated Microscopic Rate Constants[a] for the Intramolecular and Intermolecular Quenching of DBO-Labeled Peptides and DBO According to Scheme 2 in H_2O [Kinetic Solvent Deuterium Isotope Effects, i.e., $k(H_2O)/k(D_2O)$, Given in Square Brackets]

fragment	sequence	$k_+/10^6\ s^{-1}$	$k_-/10^9\ s^{-1}$	$K/10^{-3}$
upper strand	W/Y-QIFVK-DBO	9.5 [1.2]	3.2 [1.1]	3.0
lower strand	W/Y-TITLE-DBO	14.2 [1.1]	2.0 [1.0]	7.1
turn	W/Y-TLTGK-DBO	41.4 [1.2]	4.6 [1.1]	9.0
intermolecular	W/Y + QIFVK-DBO	$\equiv 3000\ M^{-1}$ [$\equiv$ 1.23]	18.6 [1.23]	160 M^{-1}

[a] The values were extrapolated by assuming an ideal intermolecular diffusion; cf. text and ref 58.

that charge effects *cannot* be responsible for the observed variations, i.e., the faster kinetics of the β-turn (TLTGK). The failure to observe a salt effect (up to 0.1 M NaCl, data not shown), which is expected to reduce electrostatic interactions by screening the charges, also supports the finding that charge effects on the end-to-end collision rate (k_+) are not well developed in our peptide sequences.

Microscopic Rate Constants for End-to-End Collision and Dissociation. We reasoned that the study of two different quenchers with varying quenching efficiency can be used to extrapolate the end-to-end collision rates and, in addition, to obtain estimates of the dissociation rates (k_- in Scheme 2) for the different peptide sequences. For fluorescence quenching of DBO, one can employ Trp as a quencher with high efficiency and Tyr as a quencher with a lower efficiency. The same results could be obtained with deprotonated Tyr (at pH 12), which is an equally efficient quencher as Trp. The end-to-end collision rates are proposed to be determined by the peptide backbone such that the rate constants for both formation as well as dissociation of the encounter complex should be the same for the DBO/Trp and DBO/Tyr pairs, i.e., $k_+^Y \approx k_+^W \equiv k_+$ and $k_-^Y \approx k_-^W \equiv k_-$. Equations 5a,b then apply for the Trp and Tyr cases as specific expressions of eq 2.

$$\text{(a) } k_q^W = \frac{k_+ k_d^W}{k_- + k_d^W} \quad \text{and} \quad \text{(b) } k_q^Y = \frac{k_+ k_d^Y}{k_- + k_d^Y} \qquad (5)$$

To solve this system of coupled equations for the respective formation and dissociation rate constants, one must specify the unimolecular rate constants for deactivation of the excited encounter complexes (k_d) for both Trp and Tyr. These rate constants should only be dependent on the quencher and therefore be independent of the chain, i.e., the same for the intramolecular and intermolecular reactions. Similar equations as in eqs 5a,b can be set up for the intermolecular cases, where k_+ adapts the meaning of a diffusion-limited rate (k_{diff}) and where k_- can be expressed through the equilibrium constant for intermolecular encounter complex formation ($k_- = K/k_{diff}$). Assuming quenching in an ideal solution without enthalpic interactions between probe and quencher, an expression for this equilibrium constant is available.[45,57] This allows one to derive values for k_d according to the resulting eqs 6a,b from the intermolecular quenching rate constants (k_q^{inter}). The diffusion-limited rate for the intermolecular reaction (k_{diff}^{inter}) was taken as $3.0 \times 10^9\ M^{-1}\ s^{-1}$ in H_2O,[58] assuming a collision radius (a) of 4 Å.[59] The values for k_d, obtained from eqs 6, amount then to $2.1 \times 10^{10}\ s^{-1}$ for Trp and $1.5 \times 10^9\ s^{-1}$ for Tyr in H_2O. In accordance with the proposed quenching mechanism, the estimated k_d values display a significant isotope effect for Tyr (1.8, hydrogen atom abstraction) but not for Trp.

$$\text{(a) } k_d^Y = \frac{3k_{diff}^{inter}\, k_q^{inter,Y}}{4000\pi a^3 N_a (k_{diff}^{inter} - k_q^{inter,Y})} \quad \text{and}$$

$$\text{(b) } k_d^W = \frac{3k_{diff}^{inter}\, k_q^{inter,W}}{4000\pi a^3 N_a (k_{diff}^{inter} - k_q^{inter,W})} \qquad (6)$$

The resulting values for k_+ and k_-, obtained by solving the system of coupled eqs 5, are entered in Table 7. While the rate constant for *intermolecular* quenching of the QIFVK-DBO peptide by Trp ($1.6 \times 10^9\ M^{-1}\ s^{-1}$) falls about a factor of 2 below the expected diffusion-limited rate ($3.0 \times 10^9\ M^{-1}\ s^{-1}$), the extrapolated end-to-end collision rate constants (Table 7) turn out to be only slightly larger than the *intramolecular* quenching rate constants for the DBO/Trp system (Table 2). The DBO/Trp probe/quencher pair is therefore well suited to assess end-to-end collision kinetics in peptides, as already projected in previous studies.[23,24] The results in Table 7 therefore support the suggestion that a reaction which is somewhat slower than diffusion-controlled in the *intermolecular* case, can become close to diffusion-controlled in the corresponding *intramolecular* system.[21,23] This is due to the decrease of the diffusion coefficient of probe and quencher when attached to the chain, which may amount to 1 order of magnitude.[21,60] The internal friction of the chain limits free diffusion, which resembles the effect of an increased viscosity in a diffusion-controlled intermolecular reaction. This diffusive effect should operate on both the formation of the encounter complex and its dissociation, since both the forward and the reverse reactions require the same conformational changes. The peptide chain will therefore not only reduce the rate of end-to-end collision (k_+) but also, in a first approximation, increase the lifetime of the encounter complex. This accounts for the observation that the k_- value decreases from $1.9 \times 10^{10}\ s^{-1}$ for the intermolecular reaction to $(2.0-4.6) \times 10^9\ s^{-1}$ for the intramolecular cases (Table 7). Note that this decrease in k_- improves the condition for

(57) Wang, X.; Bodunov, E. N.; Nau, W. M. *Opt. Spectrosc.* **2003**, *95*, 560−570.

(58) We used an empirical formula ($D = 10^{-7} \exp(\alpha - \beta \ln m)$ with m as the molecular weight) suggested for amino acids, peptides, and proteins to estimate the diffusion coefficients of QIFVK-DBO and Trp; cf. ref 21 and Creighton, T. E. *Proteins: Structures and Molecular Properties*; 2nd ed.; W. H. Freeman and Company: New York, 1993. The diffusion coefficients were then used in the Smoluchowski equation ($k_D = 4\pi N_A(r_B + r_C)(D_B + D_C)$) along with an effective reaction radius (a) of 4 Å between the reactive sites; cf. ref 59. In contrast to the use of the simple Debye−Smoluchowski equation to estimate diffusion rates ($k_{diff} = 8RT/3\eta$), this sequential treatment allows one to explicitly consider the fact that the attachment of a peptide chain to a probe or quencher will necessarily reduce its diffusion coefficient but not enhance the reaction rate, since the true reaction radius remains confined to the volume around the reactive sites of the probe and quencher itself.

(59) The collision radius (a) of 4 Å corresponds approximately to the sum of the van der Waals radii of probe (DBO) and quencher (Trp/Tyr) and is the average distance of van der Waals complexes produced by molecular dynamics simulations (M. Zacharias, D. Roccatano, unpublished results). In addition, the distance between the reactive atoms in the transition states for quenching (see Scheme 3) lies within this range.

(60) Liu, G.; Guillet, J. E. *Macromolecules* **1990**, *23*, 4292−4298.

Scheme 3. Presumed Structures for the Transition States in the Fluorescence Quenching of DBO by an Indole as a Model for Trp and by a Phenol as a Model for Tyr

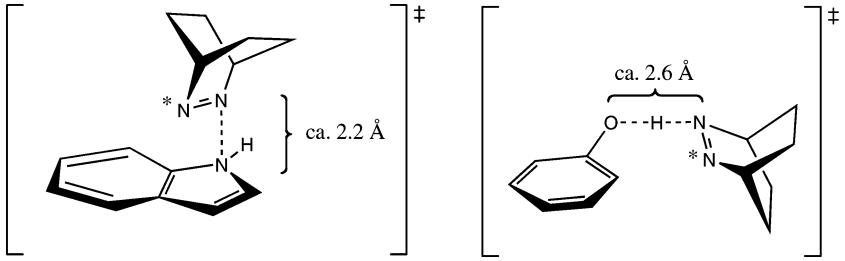

diffusion-controlled quenching in Scheme 2 ($k_d \gg k_-$), since the deactivation rate (k_d) should be independent of the attachment of the chain.

The significant variances in the rate constants for the various peptides reveal the biopolymer chains as being far from ideal, since an ideal chain would be characterized by constant values of k_+ and k_-.[45] In addition, the equilibrium constants for probe/quencher encounter complex formation ($K = k_+/k_-$, Table 7) are not constant for the different peptides. They range from 3 to 9 times 10^{-3} and fall 1 order of magnitude below the ideal expectation value[45] (ca. 0.09 for an ideal chain with 7 segments, a reaction radius of 4.0 Å,[59] and a segment length of 3.8 Å[15]). This is indicative of a slight steric repulsion between the chain ends and speaks certainly against a hydrophobic attraction and association between probe and quencher. The latter should give rise to larger values of K than for an ideal chain. For example, in a recent study employing time-resolved confocal fluorescence spectroscopy,[61] K values in the range 2.2−4.9 have been obtained for oxazine/Trp-labeled peptides, in which probe and quencher are separated by 8−9 amino acids. These are 1 order of magnitude *larger* than the ideal-chain values expected for peptides of this length (ca. 0.2 for a presumed reaction radius of 5.5 Å[62]). Indeed, a strong hydrophobic association between oxazine as probe and Trp as quencher is observed in the ground state (static quenching) and provides also a prerequisite for applying the confocal fluorescence technique, which is based on an equilibrium between two states with different fluorescence properties. In contrast, steady-state fluorescence experiments for the intramolecular and intermolecular quenching of DBO by Trp did not reveal significant static quenching,[57] which once more corroborates the absence of significant hydrophobic probe/quencher association and is in line with the very small calculated K values (Table 7).[23]

Factors Determining End-to-End Collision Rates. For peptides with Trp as quencher, the isotope effect (Table 2) on the quenching rate constants ranges from 1.1 to 1.2, which comes close to the ratio of the viscosities of D_2O and H_2O at 25 °C [$\eta(D_2O)/\eta(H_2O) = (1.1\ \text{cP})/(0.89\ \text{cP}) = 1.23$]. More significantly, there is a factor of 2−3 decrease for the end-to-end collision rates in 7.0 M guanidinium chloride solution (Table 3), which can also be accounted for in terms of the higher viscosity effect in this medium ($\eta = 1.71$ cP). In fact, the decrease is somewhat larger than expected on the basis of viscosity alone, which has been observed previously and attributed to some association of the additive to the peptide.[44] The latter is expected to cause an additional decrease of the diffusion coefficient of the chain ends.

The viscosity effects demonstrate that solvent friction is an important factor in determining the end-to-end collision rates. On the other hand, we have also evidence derived from the activation barriers (Table 3) and the large variations in end-to-end collision rate constants for different sequences (Tables 2 and 7) that the internal friction of the peptide backbone is *another* important factor. Consequently, the end-to-end collision rates in short peptides are determined by a subtle interplay between internal friction and solvent friction. The activation barriers in Table 3 suggest that end-to-end collision in the most flexible turn is mainly controlled by solvent friction; internal friction becomes sizable in the more rigid strand fragments.

Interpretation of End-to-End Collision Rates. It should be mentioned that the end-to-end collision rate in a peptide depends on the definition of what an end-to-end collision (or contact formation) actually is. The choice of the proper reaction or collision radius is particularly critical.[58] We have used a value of 4 Å for the present DBO/Trp and DBO/Tyr probe/quencher systems and the data in Table 7.[59] It can be shown that the choice of a larger radius leads to substantially higher end-to-end collision rates. It is therefore less surprising that probe/quencher systems with a larger reaction radius, like those performing exergonic triplet−triplet[63] or singlet−singlet energy transfer,[52,64] may display intramolecular quenching rate constants which are larger than those obtained from the DBO/Trp and DBO/Tyr probe/quencher pairs. Exchange energy transfer is expected to occur as soon as orbital overlap between probe and quencher is established within distances as large as 8 Å,[65−67] while quenching of DBO by Trp is subject to the stringent and proximate (≤4 Å)[59] transition state geometries for exciplex formation and hydrogen abstraction (see Scheme 3). The latter have been calculated at a very high level of theory for alcohols[68] and amines[46,69] as quenchers.

As can be seen, the quenching of DBO by Trp and Tyr requires a more intimate and better defined end-to-end contact ("a specific atom-to-atom contact") than quenching by exchange energy transfer ("a chromophore-to-chromophore orbital overlap"). Systems with a larger effective quenching radius may yield faster quenching rate constants[52,63] and therefore imply

(61) Neuweiler, H.; Schulz, A.; Boehmer, M.; Enderlein, J.; Sauer, M. *J. Am. Chem. Soc.* **2003**, *125*, 5324−5330.
(62) Vaiana, A. C.; Neuweiler, H.; Schulz, A.; Wolfrum, J.; Sauer, M.; Smith, J. C. *J. Am. Chem. Soc.* **2003**, *125*, 14564−14572.
(63) Krieger, F.; Fierz, B.; Bieri, O.; Drewello, M.; Kiefhaber, T. *J. Mol. Biol.* **2003**, *332*, 265−274.
(64) Pischel, U.; Huang, F.; Nau, W. M. *Photochem. Photobiol. Sci.* **2004**, *3*, 305−310.
(65) Nau, W. M.; Wang, X. *ChemPhysChem* **2002**, *3*, 393−398.
(66) Wagner, P. J.; Klán, P. *J. Am. Chem. Soc.* **1998**, *121*, 9626−9635.
(67) Paddon-Row, M. N. In *Stimulating Concepts in Chemistry*; Vögtle, F., Stoddart, J. F., Shibasaki, M., Eds.; Wiley-VCH: Weinheim, 2000; pp 267−291.
(68) Nau, W. M.; Greiner, G.; Rau, H.; Olivucci, M.; Robb, M. A. *Ber. Bunsen-Ges. Phys. Chem.* **1998**, *102*, 486-492.
(69) Sinicropi, A.; Pischel, U.; Basosi, R.; Nau, W. M.; Olivucci, M. *Angew. Chem., Int. Ed.* **2000**, *39*, 4582−4586.

apparently faster end-to-end collision rates, which, however, are then due to a different definition of what the "end" represents, namely an increased size of the ends. The more stringent geometric selection rules for fluorescence quenching of DBO are also reflected in the unique observation that the rates go through a maximum when the chain length is altered, i.e., the shortest homologue is *not* the fastest one.[23] While this characteristic "inversion" behavior is expected for bonding interactions in peptides,[70,71] as well as polymers,[72,73] it has not yet been reported in the related studies on polypeptides for alternative probe/quencher pairs with looser quenching geometries.[19,21,52,63]

With the important insight that there is no universal rate constant of end-to-end collision, we can return to the original motivation for measuring this quantity, which was the prediction of the rates of the elementary steps of protein folding. Clearly, the formation of initial secondary structures, whether β-turn or α-helix, requires the crucial formation of at least a single "correct" hydrogen bond, which may then lead to a zipping of the remaining parts. Hydrogen bonding presents a specific, proximate, and geometrically well-defined atom-to-atom contact, which leads us to suggest that the presently reported end-to-end collision rates present excellent estimates of the maximum rates for formation of peptide hydrogen bonds. In this context, it may or may not be important to emphasize that the atomic arrangement responsible for quenching of DBO by tyrosine with a collinear N- - -H- - -O transition state (see Scheme 3) presents an excellent mimic of the N- - -H- - -O hydrogen bond in peptides.

The present rate data suggest that the formation of the first hydrogen bond in the β-turn region can occur in as fast as 25 ns ($1/k_+$). The actual rate of formation of the entire β-hairpin cannot be directly predicted from this value alone, but it can be used as the basis to estimate the time scale. If one assumes as one extreme scenario (*i*) that each of the 6−7 important hydrogen bonds in the ubiquitin hairpin (Scheme 1a) is formed with the same rate of 25 ns (which neglects the known length dependence of end-to-end collision rates),[19,21,23] (*ii*) that exclusively correct hydrogen bonds are formed, and (*iii*) that each formation of a correct hydrogen bond leads to a rapid zipping of the two strands, one obtains a rate as fast as 4 ns for the formation of the entire β-hairpin. If, however, one makes the reasonable assumption that mismatched hydrogen bonds are also formed and that the hairpin sequence can be transiently trapped in incorrect structures, the overall process can be slowed by as much as 1−2 orders of magnitude, similar to the situation for ssDNA hairpin structures.[74] It is therefore likely that the overall rates of β-hairpin formation lie in the range of several tens to hundreds of nanoseconds, thereby approaching some early estimates.[14,16]

Conclusions

In conclusion, we have used a combination of two intramolecular probe/quencher pairs of varying efficiency, namely DBO/Trp and DBO/Tyr, to extrapolate the end-to-end collision rates in polypeptides derived from the two strand and the single turn regions of a natural β-hairpin secondary structure. The extrapolated collision rates lie close to the rates determined for the DBO/Trp pair, thereby supporting the conjectures from previous studies and confirming the notion that reactions between probe and quencher tend to become "more diffusion-controlled" upon attachment to a peptide chain as a consequence of the reduced diffusion coefficients when attached as ends to a chain. Fluorescence quenching of DBO mimics an elementary step of peptide folding, namely the formation of initial hydrogen bonds to initiate secondary structure formation, in that it involves a specific "atom-to-atom" type of collision, which is characterized by a specific transition state geometry with an intimate approach in reach of covalent bonding. The present study has also revealed that the end-to-end collision rates and thereby flexibility of peptides are highly dependent on the peptide sequence. Peptides derived from the β-turn of ubiquitin were found to be much more flexible than those of the β-strands, which exposes an important link between secondary structure propensity and elementary rate constants. Varying flexibility of peptide sequences may therefore impose a strong kinetic bias in the early stages of protein folding. The collision rate for the turn allowed an estimated rate of ca. 25 ns for the formation of a single hydrogen bond in the β-turn region. The prediction of the formation rate of an entire β-hairpin, however, does critically depend on the formation of mismatched structures, which could slow the overall process, akin to the situation for ssDNA hairpins.[74] In addition, individual amino acids were shown to have a dramatic effect on peptide flexibility through peptide "mutation" experiments, while charge repulsions or attractions between the chain ends have an insignificant effect on the end-to-end collision rates. The end-to-end collision rate constants, activation energies, and isotope effects demonstrate finally that it is a combination of internal friction in the peptide backbone (conformational changes) and solvent friction (viscosity-limited diffusion) which determines the rates of end-to-end collision in equally long peptides.

Acknowledgment. R.R.H. thanks the National Science Foundation (U.S.A.) for an International Research Fellowship (Grant INT-9901459). The study was performed within the Swiss National Research Program "Supramolecular Functional Materials" (Grant No. 4047-57552 for W.M.N.) and supported by the Schweizerischer Nationalfonds (Grant No. 620-58000 for W.M.N.). We thank Dr. K. Kulicke and Dr. G. Gramlich for assistance with the NMR measurements and Prof. J. Seelig and his group (Biozentrum, University of Basel) for help with the CD experiments.

JA0466053

(70) Mutter, M. *J. Am. Chem. Soc.* **1977**, *99*, 8307−8314.
(71) Camacho, C. J.; Thirumalai, D. *Proc. Natl. Acad. Sci. U.S.A.* **1995**, *92*, 1277−1281.
(72) Zachariasse, K. A.; Macanita, A. L.; Kuehnle, W. *J. Phys. Chem. B* **1999**, *103*, 9356−9365.
(73) Mar, A.; Fraser, S.; Winnik, M. A. *J. Am. Chem. Soc.* **1981**, *103*, 4941−4943.
(74) Wang, X.; Nau, W. M. *J. Am. Chem. Soc.* **2004**, *126*, 808−813.